Convectively coupled Rossby–Gravity waves in a field campaign: How they are captured in reanalysis products

Article *in* Atmospheric Science Letters · December 2023

DOI: 10.1002/asl.1206

Xiaocong Wang

Institute of Atmospheric Physics

Received: 21 June 2023 | Accepted: 29 November 2023
DOI: 10.1002/asl.1206

RESEARCH ARTICLE

Atmospheric Science Letters RMetS

Convectively coupled Rossby–Gravity waves in a field campaign: How they are captured in reanalysis products

Xiaocong Wang[1] | **Minghua Zhang**[2]

[1]State Key Laboratory of Numerical Modeling for Atmospheric Sciences and Geophysical Fluid Dynamics, Institute of Atmospheric Physics, Chinese Academy of Sciences, Beijing, China

[2]School of Marine and Atmospheric Sciences, Stony Brook University, Stony Brook, New York, USA

Correspondence
Xiaocong Wang, State Key Laboratory of Numerical Modeling for Atmospheric Sciences and Geophysical Fluid Dynamics, Institute of Atmospheric Physics, Chinese Academy of Sciences, Beijing 100029, China.
Email: wangxc@lasg.iap.ac.cn

Funding information
National Natural Science Foundation of China, Grant/Award Number: 42175165; Guangdong Major Project of Basic and Applied Basic Research, Grant/Award Number: 2020B0301030004; US Department of Energy; US National Science Foundation

Abstract

Convectively coupled equatorial waves are a significant source of atmospheric variability in the tropics. Current numerical models continue to struggle in simulating the coupled diabatic heating fields that are responsible for the development and maintenance of these waves. This study investigates how the diabatic fields associated with Mixed Rossby–Gravity waves (MRGs) are represented in four reanalysis products by using a unique observational dataset from the TRMM-KWAJEX (Tropical Rainfall Measuring Mission-Kwajalein Experiment) field campaign. These reanalyses include ERA5, Japanese 55-year Reanalysis (JRA-55), Climate Forecast System Reanalysis (CFSR), and Modern-Era Retrospective Analysis for Research and Applications (MERRA). We found that all four reanalyses captured the MRG structures in winds and temperature, and to a lesser degree in the humidity field except in the boundary layer. However, only the ERA5 and MERRA reanalyses captured the gradual rise and succession of the diabatic heating from boundary layer turbulence, shallow convection, cumulus congestus, and deep convection within the waves. ERA5 is the only product that also captured the gradual rise of the subgrid-scale vertical transport of moist static energy. All reanalysis products underestimated the diabatic heating from cumulus congestus. Results provide observational basis on what aspects of MRG can be trusted and what cannot in the reanalysis products.

KEYWORDS
convectively coupled equatorial waves, diabatic heating, mixed Rossby–Gravity wave, reanalysis products, TRMM-KWAJEX

1 | INTRODUCTION

Convectively coupled equatorial waves are a significant source of atmospheric variability in the tropics, which have long been recognized as fundamental building blocks of many aspects of tropical dynamics. Correctly simulating these waves remains a challenge in the modeling community. Numerical models commonly suffer from poor simulations in the wave amplitude, phase speed, and the front-to-rear tilting wave structure (e.g., Lin et al., 2006). However, the simulations have improved considerably in recent years, even though some of the biases still exist (Dias et al., 2023; Huang et al., 2013; Schreck et al., 2020). Theoretical studies have emphasized the importance of the interactions among boundary layer turbulence, shallow and deep convections, and stratiform condensation process for the simulation of these waves (Kuang, 2008; Majda & Shefter, 2001; Mapes, 2000; Wang & Li, 1993). Chikira (2010) and Park (2014), among many others, have developed cumulus parameterizations based on these ideas with some success. Although it is widely acknowledged that diabatic heating plays a crucial role in the excitation and maintenance of convectively coupled equatorial waves, numerical models usually have difficulty simulating the coupled diabatic heating fields that are responsible for the development and maintenance of these waves.

To understand how wave dynamics interact with the diabatic heating, detailed time–space distribution of the heating field and its association with the wave dynamics are desired. However, observational analysis of such time–space distribution of wave dynamics and its coupling with diabatic heating is scarce, especially for waves with time scales shorter than a few days such as the Mixed Rossby–Gravity waves (MRGs). Global reanalyses have the potential to provide such data. However, it is not clear whether they can realistically capture these waves and the associated heating fields that are significantly impacted by the physical parameterizations of the assimilation models.

The purpose of this paper is to present a critical evaluation of four widely used reanalysis products in describing convectively coupled MRG along with their associated diabatic heating fields. This is made possible by using a unique dataset from the TRMM-KWAJEX (Tropical Rainfall Measuring Mission-Kwajalein Experiment) field campaign. In the following section, we describe the data and methods. These are followed by a critical evaluation of the fidelity and limitation of different reanalysis products. The last section contains a summary.

2 | DATA AND METHODS

KWAJEX was conducted around the Kwajalein Atoll in the Republic of the Marshall Islands (7–10° N, 166–169° E) from July 24, 1999 to September 15, 1999. This is the region where MRG is climatologically most active in the tropics (e.g., Hendon & Liebmann, 1991; Kiladis et al., 2016). Six-hourly balloon soundings were made in a coordinated network of measurement stations (Figure 1a), along with other meteorological measurements from aircraft, ships, as well as remote and in situ surface-based sensors (Schumacher et al., 2007, 2008; Sobel et al., 2004; Yuter et al., 2005). Surface rain data were averaged from the gridded S-Pol radar retrievals and gauge measurements. The upper air measurements have been variationally integrated and constrained by conservations of column-integrated mass, moisture, and energy following the method of Zhang and Lin (1997) and Zhang et al. (2001). The derived Q_1 and Q_2 have been used in Schumacher et al. (2008) to match cloud observations to investigate how they are distributed in different cloud systems, and in Zhang and Hagos (2009) to investigate different modes of the diabatic heating. The analyzed vertical velocities and advective tendencies from the data also served as large-scale forcings to drive cloud-resolving models or single-column models, as in many previous studies (e.g., Blossey et al., 2007; Li et al., 2008; Wang, 2022; Wang & Zhang, 2013; Zeng et al., 2009).

By using this field campaign data, Wang and Zhang (2015) constructed a composite of the convectively coupled MRG and explored the coupling between MRG dynamics and the diabatic heating. Salient features of the coupling include the following: deep convection preceded by cumulus congestus; cumulus congestus preceded by heating and moistening from boundary layer turbulence and shallow convection; deep convection followed by stratiform-like heating in the upper troposphere and cooling in the lower troposphere; gradual rise of positive moisture anomaly and subgrid-scale vertical transport of moist static energy. Figure 1b summarizes these features along with their phase relationships with low-level horizontal winds as adapted from Wang and Zhang (2015). This composite MRG is used to assess how the reanalysis products capture the waves and their coupling with the diabatic heating.

The four reanalyses to be assessed are (1) ERA5 reanalysis (Hersbach et al., 2020) from the European Centre for Medium-Range Weather Forecasts (ECMWF); (2) Japanese 55-year Reanalysis (JRA-55, Kobayashi et al., 2015) from the Japan Meteorology Agency (JMA); (3) Climate Forecast System Reanalysis (CFSR, Saha et al., 2010) from the National Center for Environmental Prediction (NCEP); and (4) Modern-Era Retrospective Analysis for Research and Applications (MERRA, Rienecker et al., 2011) from the National Aeronautics and Space Administration (NASA). These are four widely used reanalysis products in the literature (e.g., Chen et al., 2014; Lin & Zhang, 2013). For all these reanalyses, Q_1 and Q_2 were calculated from the three-dimensional fields of winds, temperature, and moisture for the same period as the KWAJEX field campaign, and were largely influenced by the physical parameterizations of the models. All atmospheric state variables were processed to the same vertical and temporal resolution as the field campaign data. Spatial averages are done over the domain (7–10° N, 166–169° E) to mimic the size of the KWAJEX sounding network.

FIGURE 1 (a) Locations of surface and upper-air measurement stations during TRMM KWAJEX. (b) Schematics of convectively coupled MRG.

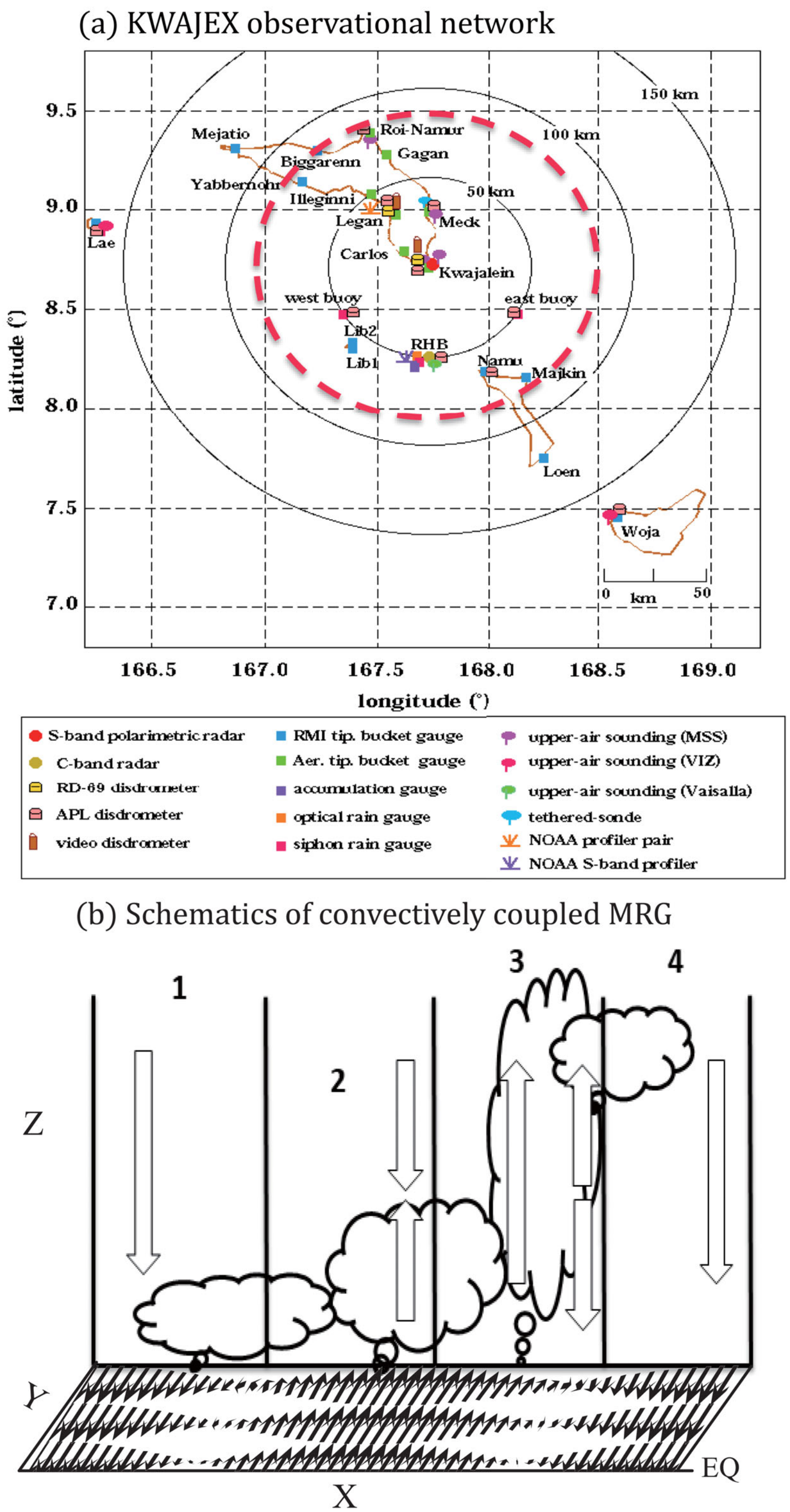

3 | RESULTS

Meridional wind is known to be a prominent signature of MRG dynamics. The time series of the 300 and 800 hPa meridional winds are shown in Figure 2a,b for the KWAJEX period in the four reanalyses along with the observation, after removal of time averages and diurnal cycles. The winds in reanalyses are all similar to each other and to the observation. They alternate from southerly to northerly every 3–6 days, as what were shown for MRG in previous studies (e.g., Aiyyer & Molinari, 2003; Liebmann & Hendon, 1990; Straub & Kiladis, 2003; Swann et al., 2006; Takayabu & Nitta, 1993). Wind directions are nearly opposite in the upper and low levels, in

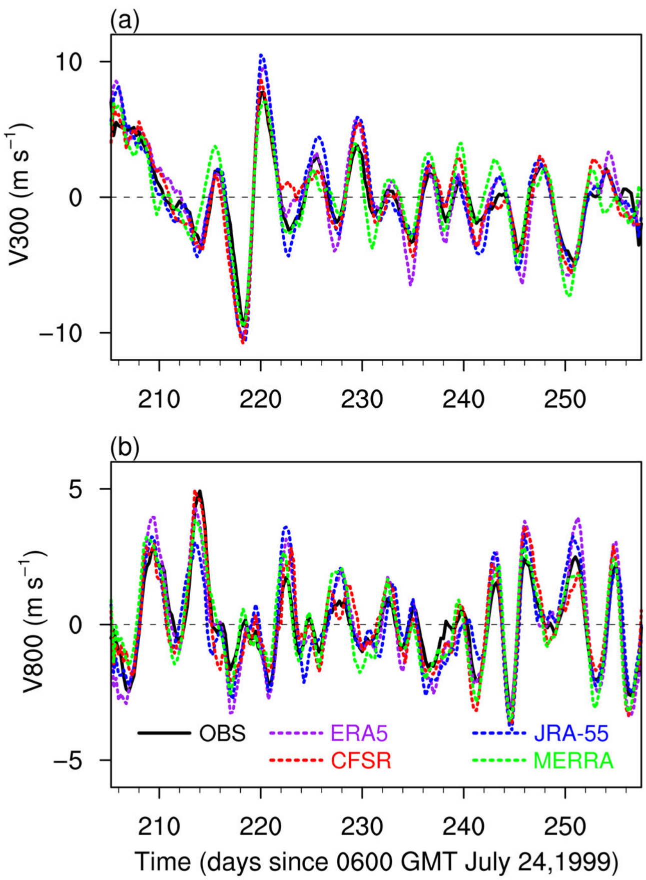

FIGURE 2 Time series of meridional wind in observation and four reanalyses at 300 hPa (a) and 800 hPa (b).

accordance with the fact that the first baroclinic mode predominates in the tropics.

The 5-day composites of the dynamic and thermodynamic fields in observations and the reanalyses are shown in Figure 3, where day 0 corresponds to the time of minima V at 300 hPa (maximum northerly). The diurnal cycle and time-averaged components have been removed in the composites. The columns from left to right are meridional wind, zonal wind, temperature, and specific humidity.

All reanalyses well captured the overall MRG wind and temperature fields. The meridional wind in the lower troposphere leads the zonal wind but lags temperature by a quarter cycle, which is manifested in all datasets and consistent with the canonical MRG dynamics (Matsuno, 1966 and Figure 1b). In the observation, an eastward tilt with height is evident in the meridional wind throughout most of the troposphere, while a westward tilt is seen above 250 hPa as in typical MRG vertical structures (Wheeler et al., 2000). All global reanalyses well reproduced these features. Their close resemblance to the observation demonstrates the quality of data assimilation in the reanalyses at the time and spatial scales of the MRG.

The resemblance is weaker in specific humidity even though the phase of the observed anomalies is, by and large, captured in all reanalyses (the rightmost column in Figure 3), for example, an eastward tilting structure with height. The observed humidity field shows a gradual rise from near the surface, to a middle level between 600 and 700 hPa, and then to a higher level between 400 and 500 hPa. Differences with the observation and among the reanalyses in the humidity field mainly lie in the lower troposphere below the level of 800 hPa preceding the arrival of the maximum low-level southerly, and in the middle troposphere between 600 and 700 hPa. CFSR well captured the two maximum centers in the middle and upper levels but underestimated the initial moistening in the boundary layer. In contrast, JRA-55 and MERRA overestimated the magnitude and altitude of the initial moisture anomaly, and underestimated the rising moistening in upper levels. Among all, ERA5 is the only product that bears close resemblance to the observation. While CFSR appears to have underestimated the mixing of moisture from the surface, JRA-55 and MERRA appear to have too strong mixing at the top of the boundary layer, either due to boundary layer turbulence or shallow convection.

Unlike the atmospheric state variables, the diagnostic fields of wind divergence and diabatic heating are not directly assimilated in the reanalyses. They are strongly impacted by the physical parameterizations of the assimilation models. The composite anomalies of wind divergence, the apparent heating (Q_1), moisture sink (Q_2), and the subgrid-scale vertical transport of moist static energy convergence are presented in Figure 4, which are put in order from left to right columns. The observations are shown in the top row.

The wind divergence field in the observation shows a gradual rise with an eastward tilting structure (Figure 4a). This gradual rise of wind convergence corresponds to the titling structure in the diabatic heating and moisture sink (Figure 4b,c). Note the peak of moisture sink is lower than that of diabatic heating, characterizing different impact of convective-scale eddy transport on heat and moisture. Heating from shallow convection precedes cumulus congestus, which is followed by deep convection and stratiform-like condensation. Such an evolution of diabatic heating during the course of MRG is schematically portrayed in Figure 1b, which is also suggested in other tropical systems (e.g., Feng et al., 2020; Straub & Kiladis, 2003).

ERA5 and MERRA are found to capture the gradual rise of the wind divergence field, and hence the titling structure in the diabatic heating and moisture sink. JRA-55 and CFSR failed to capture the coherent rising structure in the wind divergence field. This failure is then reflected in their upright structures of the diabatic

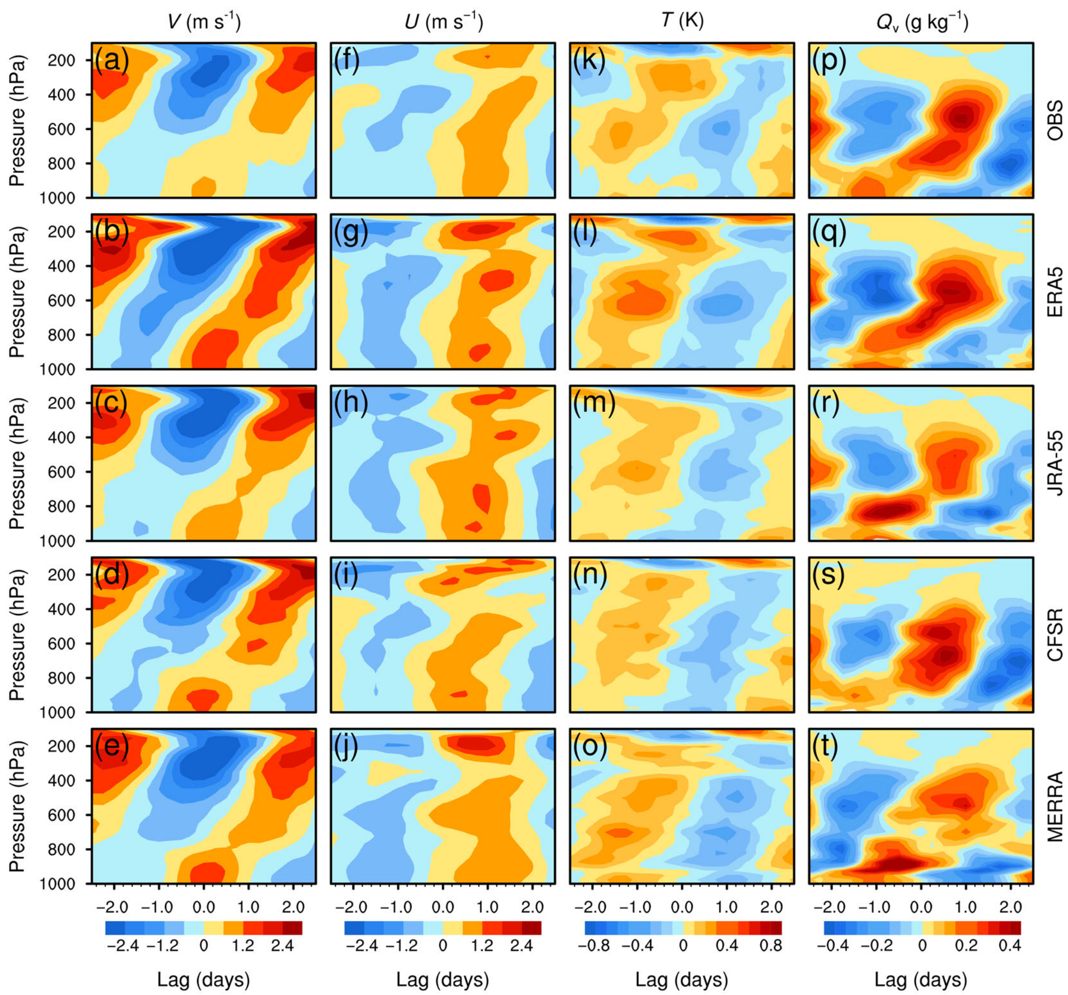

FIGURE 3 Composite of anomalies based on the minimum 300 hPa meridional wind in observation and four reanalyses. From left to the right columns are meridional wind, zonal wind, temperature, and specific humidity.

heating and moisture sink fields. The heating center that is associated with deep convection in JRA-55 and CFSR appears to occur too early. This suggests that the deep convection scheme used in the models of these two reanalyses may be triggered too easily without the need of preconditioning by the shallow and middle-level convections.

The $Q_1 - Q_2 - Q_{\mathrm{rad}}$ field describes additional details of the wave-convection coupling (Yanai et al., 1973). It equals to the tendency of moist static energy as a result of subgrid-scale vertical transport as expressed in Equation (1),

$$Q_1 - Q_2 - Q_{\mathrm{rad}} = -\frac{\partial \overline{\omega' h'}}{\partial p}, \tag{1}$$

where Q_{rad} represents radiative heating, ω' and h' are subgrid-scale anomalies of vertical velocity and moist static energy from the domain mean. As Q_{rad} anomaly is typically small because of considerable cancellation between longwave cooling and shortwave heating in the tropics (Kiehl, 1994), we use the composite anomalies of $Q_1 - Q_2$ to approximate $-\frac{\partial \overline{\omega' h'}}{\partial p}$. The observed $Q_1 - Q_2$ (Figure 4d) shows a clear eastward tilting structure, representing the increase of moist static energy by subgrid-scale vertical transport, first near the surface via boundary layer turbulent eddy, then in the lower and middle troposphere via shallow cumuli, and then in the upper troposphere by deep convection.

All reanalyses captured the initial phase of the moist static energy transport as in the observation. Differences against the observation lie in the later phases, including the magnitude of the tilted rise of $-\frac{\partial \overline{\omega' h'}}{\partial p}$. Of the four reanalyses, ERA5 best captures the observed structure. MERRA, while having a reasonable structure in Q_1, showed less organized structure in this subgrid-scale vertical transport of moist static energy. Its weaker magnitude above 500 hPa suggests that the condensational heating is more dominant there than the observation. JRA-55 and CFSR placed the upper-level convergence of moist static energy too early and

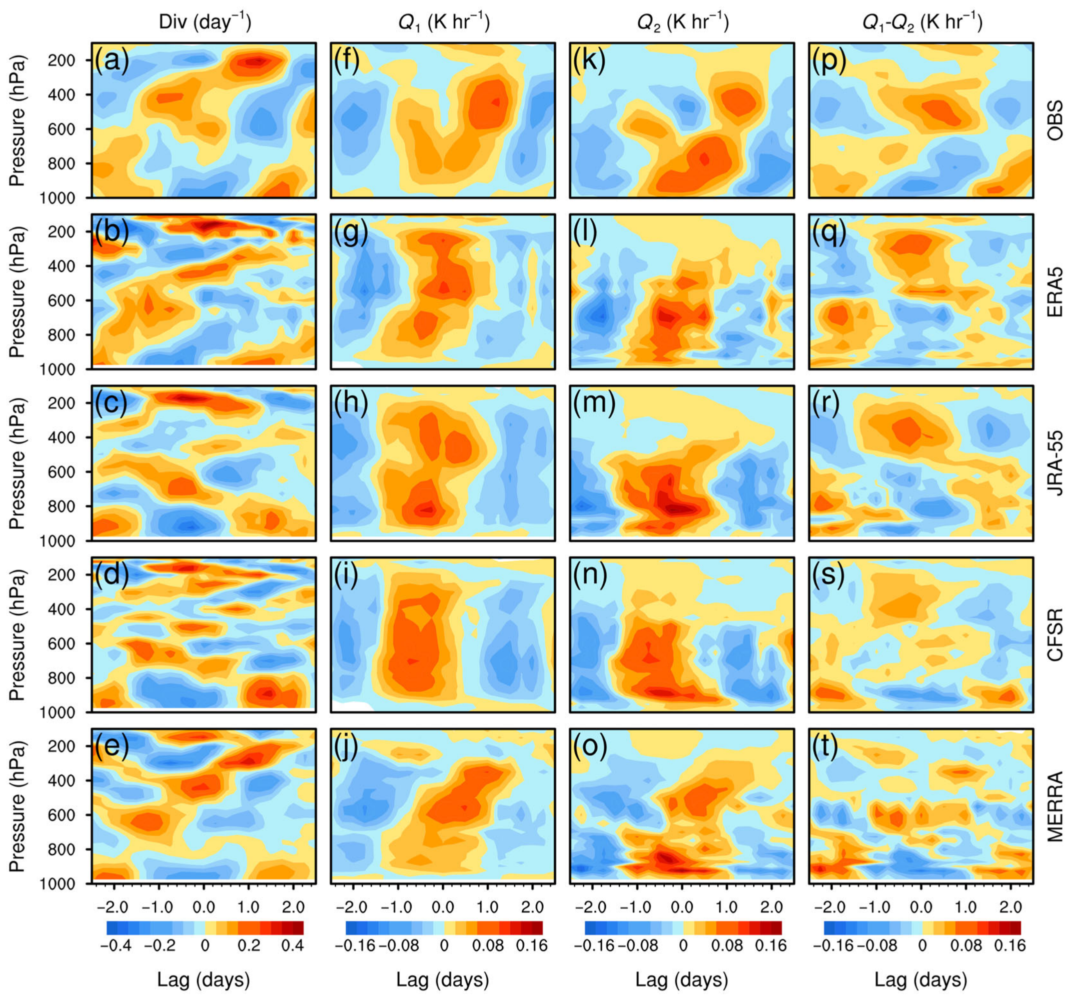

FIGURE 4 Same as Figure 3 except for the fields of wind divergence (first column), apparent heating Q_1 (second column), moisture sink Q_2 (third column), and subgrid-scale vertical transport of moist static energy convergence $Q_1 - Q_2$ (fourth column).

too high, consistent with the upright structure of diabatic heating in these two reanalyses.

One observed feature that all reanalyses failed to capture is the heating center from cumulus congestus that precedes deep convection. The observed Q_1 shows two maxima, in accordance with the surface precipitation observation, while all reanalyses only have one peak (see Figure S1). Whether the peak from cumulus congestus is essential to the development and maintenance of the MRG is not clear, but the comparison suggests that diagnostics of middle-level convection, even for ERA5, is underestimated in the reanalyses.

4 | SUMMARY AND DISCUSSION

By using the TRMM-KWAJEX field campaign data, we have evaluated the quality of four global reanalyses (ERA5, JRA-55, CFSR, and MERRA) in describing convectively coupled equatorial MRG. We have shown that all four reanalyses capture remarkably well the winds and temperature fields associated with MRG, including the alternating wind direction, and the front-to-rear tilting structures in the meridional wind and temperature. Their portrait of the moisture field is less accurate near the surface and in the lower troposphere. For the diabatic heating fields, only ERA5 and MERRA capture the observed time evolution of the vertical structure, and only ERA5 captures the correct phase of subgrid-scale vertical transport of moist static energy. All reanalyses are shown to underestimate the heating associated with cumulus congestus prior to the deep convection.

These results suggest that while the reanalyses are well suited to study the wind and temperature structures of MRG, they are less suited to study the coupled moisture and diabatic heating sources and moisture sinks within the waves. This is because, while the state variables assimilated into the assimilation systems are naturally similar to observations, the second-order fields, such as vertical velocity and diabatic heating, are not. Uncertainties in the diabatic heating fields are more likely to be caused by inadequate parameterizations of moist processes in the forecasting model. We have highlighted sources of possible model biases in the different reanalysis as a result of this evaluation, including turbulent mixing in the boundary layer too weaker in CFSR, too strong in JRA-55 and MERRA; too easy triggering of deep convection in JRA-55 and CFSR. Rigorous testing of the causes will require special numerical experiments by using the assimilation models. It is hoped that results from this study can shed some light on the basis of using or not using reanalysis products to investigate moist equatorial waves.

AUTHOR CONTRIBUTIONS

Xiaocong Wang: Formal analysis; investigation; methodology; validation; visualization; writing–original draft; writing–review and editing; funding acquisition. **Minghua Zhang**: Conceptualization; resources; visualization; writing–review and editing.

ACKNOWLEDGMENTS

The authors wish to thank Dr. Juliana Dias of NOAA and one anonymous reviewer for their constructive comments that helped to clarify and improve the original paper. Thanks also go to Dr. Courtney Schumacher of the Texas A& M University and Paul Ciesielski of Colorado State University for their help in collecting and processing the KWAJEX data that enabled the variational analysis of the diabatic heating fields used in this paper. We also thank ECMWF, JMA, NCEP, and NASA for making their reanalysis datasets ERA5, JRA-55, CFSR, and MERRA available to the public. This research is supported by the Guangdong Major Project of Basic and Applied Basic Research (Grant No. 2020B0301030004), and the National Natural Science Foundation of China under Grant 42175165. Additional support is provided by the US Department of Energy and the US National Science Foundation to the Stony Brook University.

CONFLICT OF INTEREST STATEMENT

The authors declare no conflicts of interest.

DATA AVAILABILITY STATEMENT

The analyzed campaign data in this study are available at http://cloud.somas.stonybrook.edu/mzhang/iops.

ORCID

Xiaocong Wang https://orcid.org/0000-0001-8598-1861

REFERENCES

Aiyyer, A. & Molinari, J. (2003) Evolution of mixed Rossby–Gravity waves in idealized MJO environments. *Journal of the Atmospheric Sciences*, 60, 2837–2855.

Blossey, P., Bretherton, C., Cetrone, J. & Kharoutdinov, M. (2007) Cloud-resolving model simulations of KWAJEX: model sensitivities and comparisons with satellite and radar observations. *Journal of the Atmospheric Sciences*, 64, 1488–1508.

Chen, G., Iwasaki, T., Qin, H. & Sha, W. (2014) Evaluation of the warm-season diurnal variability over East Asia in recent reanalyses JRA-55, ERA-interim, NCEP CFSR, and NASA MERRA. *Journal of Climate*, 27, 5517–5537.

Chikira, M. (2010) A cumulus parameterization with state-dependent entrainment rate. Part II. Impact on climatology in a general circulation model. *Journal of the Atmospheric Sciences*, 67, 2194–2211.

Dias, J., Gehne, M., Kiladis, G.N. & Magnusson, L. (2023) The role of convectively coupled equatorial waves in sub-seasonal predictions. *Geophysical Research Letters*, 50, 1–10.

Feng, T., Yu, J., Yang, X. & Huang, R. (2020) Convective coupling in tropical-depression-type waves. Part II: Moisture and moist static energy budgets. *Journal of the Atmospheric Sciences*, 77(10), 3423–3440. Available from: https://doi.org/10.1175/JAS-D-19-0173.1

Hendon, H. & Liebmann, B. (1991) The structure and annual variation of antisymmetric fluctuation of tropical convection and their association with Rossby–Gravity waves. *Journal of the Atmospheric Sciences*, 48, 2127–2140.

Hersbach, H., Bell, B., Berrisford, P., Hirahara, S., Horanyi, A., Munoz-Sabater, J. et al. (2020) The ERA5 global reanalysis. *Quarterly Journal of the Royal Meteorological Society*, 146, 1999–2049.

Hung, M.-P., Lin, J.-L., Wang, W., Kim, D., Shinoda, T. & Weaver, S.J. (2013) MJO and convectively coupled equatorial waves simulated by CMIP5 climate models. *Journal of Climate*, 26(17), 6185–6214.

Kiehl, J.T. (1994) On the observed near cancellation between longwave and shortwave cloud forcing in tropical regions. *Journal of Climate*, 7, 559–565.

Kiladis, G.N., Dias, J. & Gehne, M. (2016) The relationship between equatorial mixed Rossby–Gravity and eastward Inertio-gravity waves. Part I. *Journal of the Atmospheric Sciences*, 73, 2123–2145.

Kobayashi, S., Ota, Y., Harada, Y., Ebita, A., Moriya, M., Onoda, H. et al. (2015) The JRA-55 reanalysis: general specifications and basic characteristics. *Journal of the Meteorological Society of Japan Series II*, 93, 5–48.

Kuang, Z. (2008) A moisture-stratiform instability for convectively coupled waves. *Journal of the Atmospheric Sciences*, 65, 834–854.

Li, Y., Zipser, E., Krueger, S. & Zulauf, M. (2008) Cloud-resolving modeling of deep convection during KWAJEX. Part I. Comparison to TRMM satellite and ground-based radar observations. *Monthly Weather Review*, 136, 2699–2712.

Liebmann, B. & Hendon, H. (1990) Synoptic-scale disturbances near the equator. *Journal of the Atmospheric Sciences*, 47, 1463–1479.

Lin, J., Kiladis, G., Mapes, B., Weickmann, K., Sperber, K., Lin, W. et al. (2006) Tropical intraseasonal variability in 14 IPCC AR4 climate models. Part I. Convective signals. *Journal of Climate*, 19, 2665–2690.

Lin, J. & Zhang, C. (2013) Diabatic heating profiles in recent global reanalyses. *Journal of Climate*, 26, 3307–3325.

Majda, A. & Shefter, M. (2001) Models for stratiform instability and convectively coupled waves. *Journal of the Atmospheric Sciences*, 58, 1567–1584.

Mapes, B. (2000) Convective inhibition, subgrid-scale triggering energy, and stratiform instability in a toy tropical wave model. *Journal of the Atmospheric Sciences*, 57, 1515–1535.

Matsuno, T. (1966) Quasi-geostrophic motions in the equatorial area. *Journal of the Meteorological Society of Japan*, 44, 25–43.

Park, S. (2014) A unified convection scheme (UNICON). Part II. Simulation. *Journal of the Atmospheric Sciences*, 71, 3931–3973.

Rienecker, M., Suarez, M., Gealro, R., Todling, R., Bacmeister, J., Liu, E. et al. (2011) MERRA: NASA's modern-era retrospective analysis for research and applications. *Journal of Climate*, 24, 3624–3648.

Saha, S., Moorthi, S., Pan, H., Wu, X., Wang, J. & Nadiga, S. (2010) The NCEP climate forecast system reanalysis. *Bulletin of American Meteorological Society*, 91, 1015–1057.

Schreck, C.J., Janiga, M.A. & Baxter, S. (2020) Sources of tropical subseasonal skill in the CFSv2. *Monthly Weather Review*, 148(4), 1553–1565.

Schumacher, C., Ciesielski, P. & Zhang, M. (2008) Tropical cloud heating profiles: analysis from KWAJEX. *Monthly Weather Review*, 136, 4289–4300.

Schumacher, C., Zhang, M. & Ciesielski, P. (2007) Heating structures of the TRMM field campaigns. *Journal of the Atmospheric Sciences*, 64, 2593–2610.

Sobel, A., Yuter, S., Bretherton, C. & Kiladis, G. (2004) Large-scale meteorology and deep convection during TRMM KWAJEX. *Monthly Weather Review*, 132, 422–444.

Straub, K. & Kiladis, G. (2003) The observed structure of convectively coupled Kelvin waves: comparison with simple models of coupled wave instability. *Journal of the Atmospheric Sciences*, 60, 1655–1668.

Swann, A., Sobel, A., Yuter, S. & Kiladis, G. (2006) Observed radar reflectivity in convectively coupled Kelvin and mixed Rossby-Gravity waves. *Geophysical Research Letters*, 33, 1–4.

Takayabu, Y. & Nitta, T. (1993) 3–5 day-period disturbances coupled with convection over the tropical Pacific Ocean. *Journal of the Meteorological Society of Japan*, 71, 221–246.

Wang, B. & Li, T. (1993) A simple tropical atmospheric model of relevance to short-term climate variation. *Journal of the Atmospheric Sciences*, 50, 260–284.

Wang, X. (2022) Role of cloud subgrid-scale structure in modulating clouds viewed by ISCCP, MODIS, and MISR simulators. *Journal of Geophysical Research: Atmospheres*, 127, e2021JD036378. Available from: https://doi.org/10.1029/2021JD036378

Wang, X. & Zhang, M. (2013) An analysis of parameterization interactions and sensitivity of single-column model simulations to convection schemes in CAM4 and CAM5. *Journal of Geophysical Research*, 118, 1–12.

Wang, X. & Zhang, M. (2015) The coupling of mixed Rossby-Gravity waves with diabatic heating during the TRMM KWAJEX field campaign. *Geophysical Research Letters*, 42, 1–9.

Wheeler, M., Kiladis, G. & Webster, P. (2000) Large-scale dynamical fields associated with convectively coupled equatorial waves. *Journal of the Atmospheric Sciences*, 57, 613–640.

Yanai, M., Esbensen, S. & Chu, J. (1973) Determination of bulk properties of tropical cloud clusters from large-scale heat and moisture budgets. *Journal of the Atmospheric Sciences*, 30, 611–627.

Yuter, S., Houze, R., Smith, E., Wilheit, T. & Zipser, E. (2005) Physical characterization of tropical oceanic convection observed in KWAJEX. *Journal of Applied Meteorology*, 44, 385–415.

Zeng, X., Tao, W., Zhang, M., Hou, A., Xie, S., Lang, S. et al. (2009) A contribution by ice nuclei to global warming. *Quarterly Journal of the Royal Meteorological Society*, 135, 1614–1629.

Zhang, C. & Hagos, S. (2009) Bi-modal structure and variability of large-scale diabatic heating in the tropics. *Journal of the Atmospheric Sciences*, 66, 3621–3640.

Zhang, M. & Lin, J. (1997) Constrained variational analysis of sounding data based on column-integrated budgets of mass, heat, moisture, and momentum: approach and application to ARM measurements. *Journal of the Atmospheric Sciences*, 54, 1503–1524.

Zhang, M., Lin, J., Cederwall, R., Yio, J. & Xie, S. (2001) Objective analysis of ARM IOP data: method and sensitivity. *Monthly Weather Review*, 129, 295–311.

SUPPORTING INFORMATION

Additional supporting information can be found online in the Supporting Information section at the end of this article.

How to cite this article: Wang, X., & Zhang, M. (2023). Convectively coupled Rossby–Gravity waves in a field campaign: How they are captured in reanalysis products. *Atmospheric Science Letters*, e1206. https://doi.org/10.1002/asl.1206